



Original Paper

Gas Emission and Soil Chemical Properties Associated with Underground Coal Fires, Wuda Coalfield, Inner Mongolia, China

Haiyan Wang,¹ Junpeng Zhang ,^{1,2} Lei Zhang,¹ Jiali Wang,¹ and Zuohui Xu¹

Received 6 March 2020; accepted 4 May 2020
Published online: 23 May 2020

The coal fire area in the Wuda coalfield is divided into four parts based on the degree of burning and on surface characteristics: sub-area B is characterized by degraded vegetation, sub-area A has spontaneous combustion but no obvious features, sub-area O has vents and cracks, and sub-area C is characterized by red pyro-metamorphic rocks. Emitted gas contents and temperature at the surface were measured and analyzed. In addition, soil samples were collected for analysis of chemical soil properties. The compositions and concentrations of emitted gases vary from one sub-area to another. The nearly the same correlations among gas contents in sub-area A and in sub-area O indicate that their generation mechanism is the same. SO₂, H₂S, C₂H₆, C₂H₄, and C₂H₂ can only be detected near the cracks and vents in sub-area O. CO and H₂ can still be detected in sub-area C, although the CO₂ and CH₄ contents in sub-area B are higher. Sub-areas A and B exhibit high organic matter contents due to plant nutrient accumulation and deposition of plant litter, whereas organic matter contents decrease at the vents and cracks in sub-area O and in sub-area C because of pyrolysis, leaching, and erosion. Soil near the vents and cracks in sub-area O show strong acidity, and soil pH is correlated with total salt contents of soil, which are composed mainly of Al-, K-, Mg-, or Fe-bearing sulfates. Sub-area A showed weak soil acidity, which was the result of acidification of pore water in soil due to their long-term exposure to CO₂ and SO₂. Total salt contents in soil in the coal fire area show no significant difference compared to those in the background area except near the vents and cracks in sub-area O. The findings of this study suggest that gas emission and soil chemical properties are reliably related to the underground coal fires.

KEY WORDS: Coal seam fire, Wuda coalfield, Emitted gas, Soil chemical properties.

INTRODUCTION

Underground coal fires are an environmental catastrophic disaster. They occur commonly when underground or exposed coal seams are long-term

exposed to the air, and as heat accumulates due to exothermic reactions, they ignite and finally burn when the temperature of coal accumulation exceeds approximately 80 °C (Stracher and Taylor 2004; Kuenzer et al. 2007; Song et al. 2015). Underground coal fires are a global catastrophe. They have been reported in China, the USA, India, Indonesia, Australia, South Africa, Russia, Croatia, and other countries (Sokol et al. 2014; Song and Kuenzer 2014, 2017). Coal fires burn out nonrenewable coal re-

¹School of Emergency Management and Safety Engineering, China University of Mining & Technology, Beijing, Beijing 100083, China.

²To whom correspondence should be addressed; e-mail: sdbzzjp@126.com

sources and release tremendous amount of toxic gases (e.g., CO and SO₂), greenhouse gases (e.g., CO₂ and CH₄), and trace elements (e.g., As, F, and Hg) (Carras et al. 2009; Song et al. 2019). They also cause land subsidence (Kuenzer and Stracher 2012) and a decrease in vegetation density (Kuenzer et al. 2007), which endanger the health of local residents as well as the ecological environment (Melody and Johnston 2015).

Gas and particulate emissions from underground coal fires occur by two ways (Engle et al. 2011): (1) advective and convection transport through vents and cracks and (2) diffusion upward from the soil. Up to now, research on gas and particulate emissions has focused on vents and other surface openings during intense combustion of coal fire (Hower et al. 2009, 2013; O'Keefe et al. 2010, 2018; Engle et al. 2011; Wang et al. 2017a, b; Garrison et al. 2017). However, few comparisons have been made regarding differences in gas compositions and concentrations of different surface features caused by underground coal fires. Besides gas-phase products, underground coal fires may have effects on soil chemical properties.

Chemical and mineralogical changes in soils can be induced by the presence of gases emitted from the underground. For example, CO₂ in soil dissolves and reacts with soil water and forms carbonic acid (H₂CO₃). Decrease in soil pH has been treated as a primary parameter indicating CO₂ intrusion into soil in carbon capture and storage (CCS) studies (Harvey et al. 2013). In addition, convective heat emitted together gases directly affects soil properties. Similarly due to forest fires, soil pH is increased by soil heating due to organic acid denaturation, and severe fires can cause a significant removal of organic matter (Certini 2005). Zeng et al. (2018) revealed that the thermal effect of coal fire has changed soil properties in the Daquanhu coal fire, Xinjiang region, and concluded that thermal effect of coal fire can digest organic matter, resulting in increase in alkaline matter. Wang et al. (2019) found that released particles might enrich organic matter, and that underground coal fires affect the distribution of metal in soil. Zhang et al. (2013) found underground coal fires significantly influence soil pH, moisture, and NO₃⁻ content around gas vents in the MaNasi county of Xinjiang, China, but have little effect on other elements, organic matter, and available nutrients. Gas anomalies can also affect the redistribution of soil microbial community, indirectly leading to change in physicochemical properties of soil. In

geochemical exploration, changes in physicochemical properties of soil (e.g., pH, electrical conductivity (EC), oxidation–reduction potential (Eh), organic matter) induced by long-term seepage of hydrocarbons have been used as potential indicator of petroleum accumulation at deeper levels (Rasheed et al. 2013; Xu et al. 2017). Therefore, anomalies of surface soil properties can be related reliably to underground coal fires. However, the effect of underground coal fires on soil properties has not been comparatively investigated in different surface states, and the relationship between emitted gas compositions and soil chemical properties has not been studied extensively.

The aims of the investigation were fourfold. (1) To determine the near-surface gas composition and concentration of the coal fire areas featured with different surface characteristics. (2) To collect surface soils and analyze soil organic matter, soil pH, and total salt contents. (3) To map the distribution of surface temperature, soil organic matter, and soil pH. (4) To apply statistical tools to investigate the effect of underground coal fires on soil properties and on the distribution of emitted gas.

MATERIALS AND METHODS

Study Areas

The Wuda coalfield (39° 27' 00"–39° 34' 04" N, 106° 34' 41" E–106° 38' 41" E) is located in the west of Wuhai City, Inner Mongolia Autonomous Region, northern China. It covers an area of 35 km², and it borders to the Gobi Desert in the west and north, and to the Yellow River and Ordos Loess Plateau in the east. It includes three coal mines: Wuhushan, Suhaitu, and Huangbaici (Fig. 1). The mean altitude is ~1200 m with prevailing northwesterly wind (Shan et al. 2019). It is rich in Carboniferous-Permian coal, with over 16 minable seams and a reserve of 660 million tons, and produces mainly bituminous coal with sulfur content of up to 3.42% (Dai et al. 2002). The area has suffered badly from coal fires for > 50 years. Fire-extinguishing projects have been carried out to suppress the coal fires in the last decade, but underground fires still occur and endanger the ecological environment (Shan et al. 2019).

This study targeted two areas: coal fire area (39° 32' 23.67" N, 106° 38' 03.45" E) and background area (39° 32' 19.28" N, 106° 37' 56.92" E) (Fig. 2).

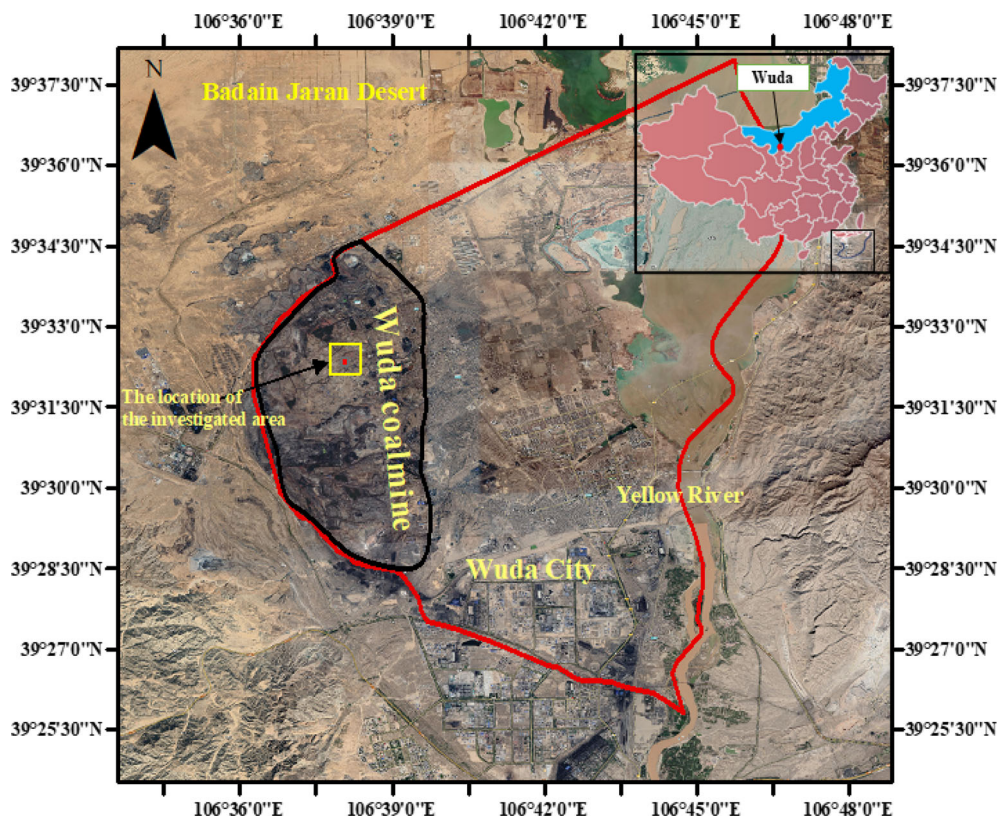


Figure 1. Location of the studied coal fire area in the Wuda coalfield, Inner Mongolia, China.

Coal fire area II is a waste mining pit, and the abandoned wellhead is visible on the ground (Fig. 3I). The abandoned wellhead exacerbates the fire's spread to the west, because the oxygen penetrates into the burning area from it. The area is an original landscape without landfill, covered with a thin layer (< 0.3 m thick) of soil. Coal fire area II is divided into sub-areas A, B, C, and O based on combustion degree and surface characteristics. The landscape of the coal fire area is shown in Figure 3.

All the vents and cracks measured in the coal fire area were in sub-area O. The ground surface of the coal fire is a 5-m-thick limestone layer, and the underlying coal seam is the 4-m-thick No. 10 coal seam, which has been ignited. Surface cracks and vents without fumes crossed each other to form a burning surface, and mineral condensation/precipitation occurred within the mouth of vent and cracks (Fig. 3O). The surface is obviously whiter than other places, as can be seen from Google maps (Fig. 2), which indicates that the coal fires have been in the stage of intense combustion for a long time. Sub-

area A refers to the vicinity of the vents and cracks but with no obvious features. Sub-area C is located northeast of the coal fire area, where subsidence exists due to the underground coal fires, and red pyro-metamorphic rocks can be seen on the ground (Fig. 3C), which indicate that the coal fire is nearing the end of its life span. Sub-area B is located at periphery of sub-area A, where degraded weeds are scattered (Fig. 3B). The background area (I) is located west of the coal fire area, about 0.3 km away, where there is a man-made pit for cutting off the spread of underground coal fires between the two areas. Sparse green weeds are scattered in the background area (Fig. 3II), which indicates that the area is not yet affected by the coal fire.

Soil Sampling

The surface survey of the coal fire area was conducted in August 2019. Samples were collected from sub-area A at closely spaced intervals with a

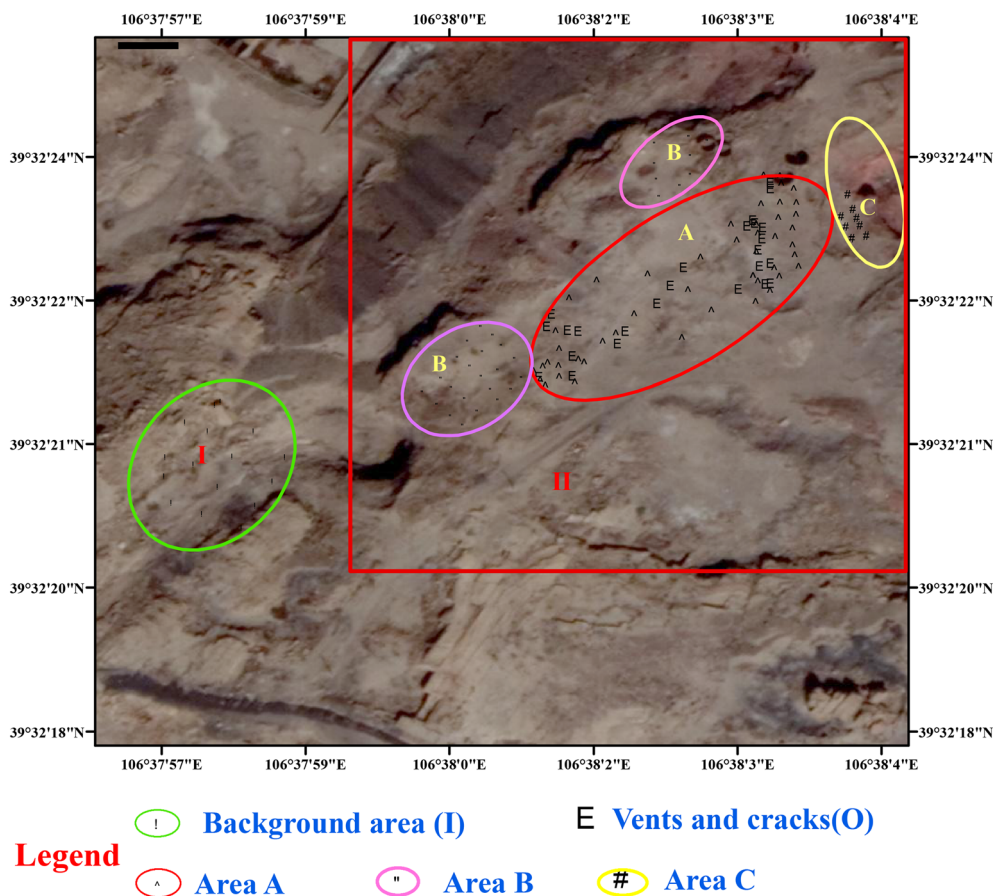


Figure 2. Location of soil and gas sampling points.

mean distance of approximately 5 m. At each grid point, surface soils with depth of 0.3 cm within 10 cm radius were collected to one sample using the Teflon tool. At the same time, the coordinates of each sampling point were recorded. In total, 26 cracks and vents were found in the coal fire area (Fig. 3), and soil beside cracks and vents were collected. A 5 m × 5 m grid was also mapped in sub-area B, where 31 representative samples were collected. Eight samples of surface soil were collected from sub-area C using the same method. A 10 m × 10 m grid was mapped in the background area, where 16 representative samples were collected. The distributions of the sampling points are shown in Figure 2. All the collected soil samples were stored in polyethylene bags and then transported to the laboratory. Later, the samples were

air-dried, milled, and sieved through a 2-mm sieve for the tests.

Surface Gas Concentration Measurement

At each soil sampling point, a corresponding gas sampling measurement was taken. On-site monitoring for H₂S, SO₂, and H₂ was performed using a portable gas analyzer with self-priming pump (SKY6000, Yuante Shenzhen). The measurement accuracy was ± 5–20%, depending on the concentration range. The probe was hammered down to a depth of approximately 5 cm at each grid point, and the sampling device was connected to a rubber tube attached to the gas inlet of the analyzer. The instrument was set to collect above-gas concentra-



Figure 3. Landscapes above underground coal fires in the investigated areas.

tion data every 1 s within a measurement duration of 2 min, and the data were recorded until data display was stable during the measurement process. At the same time, gas was drawn with a gas-tight syringe and injected into a clean aluminum foil sampling bag. All the air-tight bags with gas samples were transferred to the laboratory within 24 h. Then, concentrations of emitted gas, including CO, CO₂, CH₄, C₂H₆, C₂H₄, and C₂H₂, were analyzed using a capillary gas chromatograph (GC-4000A, Beijing) with a thermal conductivity detector (TCD). The principal statistical parameters of the data in the investigated sub-area A are given in Table 2, and the Pearson correlation coefficients of the principal parameters were calculated using SPSS22.0 (Table 1).

Soil Chemical Analyses

Soil pH was measured when the ratio of soil to water was 1:2.5 (weight:weight). A mixture of 10 g air-dried soil sample and 25 ml of deionized water was shaken together for 1 h and allowed to settle for 2 h; then, soil pH determined using a pH meter (provided by Mettler-Toledo Company). Organic matter content was measured by potassium dichromate oxidation. The distribution of soil pH and or-

ganic matter content in the investigated areas were interpolated using inverse distance weighting method in ArcGIS 10.4 (Figs. 5 and 6). Total soil salt content was determined by measuring the electrical conductivity of soil leaching solution.

Temperature Measurement

An infrared thermal imager (Fortric220s, America) was used to measure surface temperature during the soil sample collection. The range and accuracy of the imager are -20 to 150 °C and $\pm 0.2\%$. The temperature distribution can be seen clearly from the images (e.g., Fig. 4 vent). The highest temperature in the image was selected as representative temperature. The surface temperature data were interpolated using inverse distance weighting method in ArcGIS 10.4 (Fig. 4).

Statistical Analysis

A statistical t-test was used to determine statistically whether the mean concentrations of soil organic matter content, mean soil pH, and mean total salt content in the different (sub-)areas were significant ($p \leq 0.01$).

Table 1. Pearson correlation coefficients of principal components analyzed in the coal fire area

Components	Temperature	CO ₂	CO	CH ₄	H ₂	H ₂ S
CO ₂	0.84** (O) 0.194 (A) - 0.145 (B)	1				
CO	0.575 (O) 0.195 (A) - 0.126 (B)	0.799** (O) 0.943** (A) 0.155 (B)	1			
CH ₄	0.789** (O) 0.255 (A) - 0.557 (B)	0.815** (O) 0.679** (A) 0.613** (B)	0.760** (O) 0.719** (A) 0.345 (B)	1		
H ₂	0.909** (O) 0.253 (A)	0.871** (O) 0.773** (A)	0.606* (O) 0.871** (A)	0.746** (O) 0.837** (A)	1	
H ₂ S	0.685** (O) 0.286 (A)	0.834** (O) 0.720** (A)	0.716** (O) 0.675** (A)	0.724** (O) 0.572** (A)	0.757** (O) 0.806** (A)	1
SO ₂	0.763** (O) 0.105 (A)	0.788** (O) 0.907** (A)	0.788** (O) 0.804** (A)	0.645** (O) 0.678** (A)	0.813** (O) 0.864** (A)	0.809** (O) 0.852** (A)

Letters in parenthesis denote sub-areas in the coal fire area

**Significant difference at $p = 0.01$

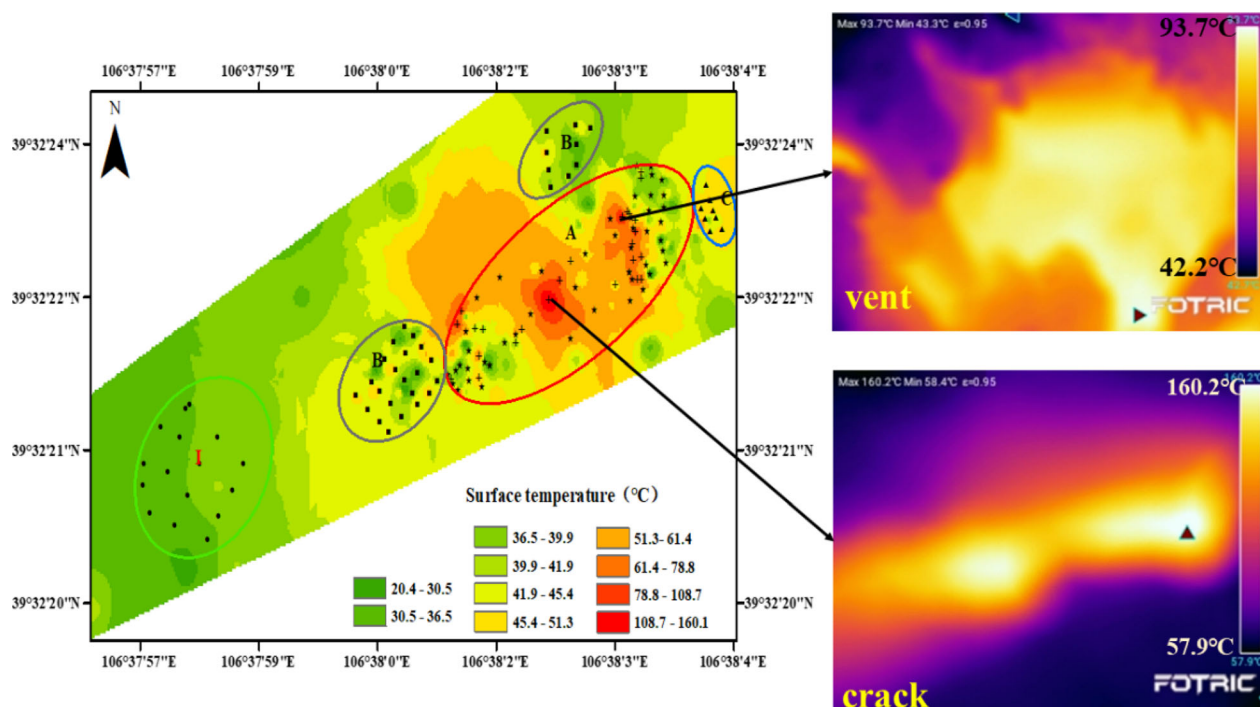


Figure 4. Distribution of surface temperature in the investigated area.

Table 2. Principal statistical parameters of multiple gases in the investigated area

Site	Statistical parameters	Surface temp. (°C)	CO ₂ (ppm)	CO (ppm)	CH ₄ (ppm)	H ₂ (ppm)	C ₂ H ₆ (ppm)	C ₂ H ₄ (ppm)	C ₂ H ₂ (ppm)	SO ₂ (ppm)	H ₂ S (ppm)	CO ₂ /CO
Background area (I)	Minimum	26	666	8.14	2.4	Bdl	Bdl	Bdl	Bdl	Bdl	Bdl	–
	Maximum	41	1088	13	4.8	Bdl	Bdl	Bdl	Bdl	Bdl	Bdl	–
	Mean	35.4	812	10.6	3.0	–	–	–	–	–	–	–
	Standard deviation	4.4	134	1.2	0.6	–	–	–	–	–	–	–
	Percentage of samples*	100	100	75	75	–	–	–	–	–	–	–
Vents and cracks (O)	Minimum	39	17433	280	102	170	10.63	29.54	Bdl	8	1	42.3
	Maximum	162	45267	890	758	1856	26.43	34.5	Bdl	30	38	88.6
	Mean	77	34603	561.4	436.5	930	16.10	32.06	–	19	23	63.3
	Standard deviation	39.4	7354	196.8	224.1	453	8.95	3.5	–	6	11	13.5
	Percentage of samples*	100	100	100	100	100	100	100	–	100	100	100
Sub-area A	Minimum	19.4	5834	166	21	3	5.80	5.41	5.05	1.3	1	20.55
	Maximum	71.7	46304	990	762	1410	30.76	9.13	Bdl	18	33	72.5
	Mean	44.9	21908	477	282.6	472	15.63	7.27	–	8	12	44.48
	Standard deviation	13.4	11700	257.4	220.9	396	10.12	2.62	–	5	9	12
	Percentage of samples*	100	100	100	100	100	23.3	6.7	3.3	93	83	100
Sub-area B	Minimum	28.4	923	8.69	2	Bdl	Bdl	Bdl	Bdl	Bdl	Bdl	11
	Maximum	51.9	14012	72.8	73	Bdl	Bdl	Bdl	Bdl	Bdl	Bdl	1517
	Mean	42.3	5037	17.7	16.9	–	–	–	–	–	–	328.38
	Standard deviation	6.2	3507	15.3	21.2	–	–	–	–	–	–	379
	Percentage of samples*	100	100	100	100	–	–	–	–	–	–	100
Sub-area C	Minimum	38	1026	10	2.15	11	Bdl	Bdl	Bdl	Bdl	Bdl	4.7
	Maximum	59	1677	89	11.6	100	Bdl	Bdl	Bdl	Bdl	Bdl	84
	Mean	46.8	1387	38	5.3	50	–	–	–	–	–	26.9
	Standard deviation	7.2	230	5.3	3.8	37	–	–	–	–	–	25.4
	Percentage of samples*	100	100	100	100	50	–	–	–	–	–	100

*Percentage of samples: gas samples with concentration of a given component over all samples

Bdl Below detection limit

RESULTS AND DISCUSSION

Analysis of Surface Temperature and Emitted Gas

Most of the temperature measurements were taken during daytime when the surface soil was warmed by solar heating. Nearly all the abnormal red parts correspond to cracks and vents (Fig. 4). The maximum temperature at the mouth of cracks is 162 °C. The mean temperature at vents and cracks is 77 °C, and it is significantly higher than in sub-area A (Table 2). The mean temperature in sub-area A is 44.9 °C, mostly falling into the range of 45.4–61.4 °C (Fig. 4), and it is significantly lower than at vents and cracks. This indicates that thermal surface anomalies

are dominated mainly by the vents and cracks. Heat is transferred via vents and cracks to the overlying bedrock, and the slow conductive heat underground can be masked by solar heating during the day (Zhang and Kuenzer 2007). As for sub-area C, the temperature ranges from 39.9 to 45.4 °C, which is slightly higher than in the background area (Fig. 4).

The probe was unable to penetrate into the rock in sub-area A, and so the gas samples were collected mainly from the soil. The contents of emitted gas in sub-area A are slightly lower than at vents and cracks, while soil composition in sub-area A is the same as at vents and cracks. This proves that gas can rise along faults to the overlying bedrock from the high-temperature zone below and exist in soils as

adsorption or free state because of long-term seepage. The emitted gas contents correlate with the temperature at the vents and cracks, while there is almost no correlation between gas content and surface temperature in sub-area A (Table 1), where surface temperature is masked by heating solar. To investigate further the correlation between gas content and surface temperature, measurements should be taken during winter or at dawn to avoid solar heating (Carras et al. 2009). However, the degree of fracture development in the overlying strata influences gas migration. The concentration of gas is high in the zones of dense fissures and tectonic discontinuities within the strata formations, confirming the large variation of gas contents (Table 2). It should be noted that the correlations among gases in sub-area A are similar, and even higher, compared to those at vents and cracks. This indicates that the emitted gases in sub-area A and at the vents and cracks have a common source, and likely originates from coal combustion. In other words, emitted gases in sub-area A can also indicate the degree of combustion in underground coal fires based on mutual correlations among the gases.

CO₂, CO, CH₄, and H₂ are dominant in sub-area A and at vents and cracks. Their contents in soil exhibit large variation, and their influential factors include fire depth, ventilation in the area, and relative position of the fire front (Song et al. 2020a, b). Moderate correlations of CO₂ and H₂ contents with surface temperature indicate that CO₂ and H₂ contents are the most impacted by vent/crack temperatures (Table 1). The CO contents have no correlation with temperature, and this indicates that the rates of CO production and loss appear to be influenced by other factors. The mean H₂ concentration at vents/cracks and in sub-area A is 566 ppm and 477 ppm, respectively (Table 1). The higher H₂ contents indicate that the coal is in a period of transition from the semi-coke to the coke in sub-area A (Zhang et al. 2008). Wang et al. (2017a, b) found that H₂ is released slowly and cannot even be detected when coal temperature is < 100 °C, but is generated in large amounts at high temperatures (> 400 °C) by coal pyrolysis. Therefore, higher H₂ contents also indicate that underground coal fires are in an advanced heating phase. The mean contents of SO₂ and H₂S at vents and cracks are 19 ppm and 23 ppm, respectively. Contents of C₂H₆, C₂H₄, and C₂H₂ were detected only in trace amounts in soil in sub-area A: < 23.3%, 6.7%, and 3.3%, respectively (Table 2).

Contents of CO₂ and CH₄ in soil in sub-area C are nearly equal to those in the background area, while the mean of CO and H₂ contents in the former is higher than in the latter (Table 2). These indicate that the underground coal fire is not extinct completely. As for sub-area B, the mean CO content is slightly higher than in the background area. The means of CO₂ and CH₄ contents (5037 ppm and 16.9 ppm, respectively) in sub-area B are significantly higher than in the background area (Table 2). However, other gases including H₂, H₂S, SO₂, C₂H₆, C₂H₄, and C₂H₂ were not detected in sub-area B. Only a weak correlation was found between CO₂ and CH₄ contents in sub-area B ($R = 0.613$, $p < 0.01$), which is smaller than in sub-area A. In addition, CO₂ and CH₄ have no correlation with the CO contents, indicating that CO₂ and CH₄ may not originate from one source, but may have partly generated from microbial activity because of the enriched humus on the surface (Sechman et al. 2013).

The volume ratio of CO₂/CO also varies among the investigated areas. In sub-area B, the mean CO₂/CO ratio of ~ 300 is very high because the CO concentration is relatively lower. When the underground coal fires enter the high oxidation regime, the CO₂/CO ratio approaches ~ 50 because more CO is produced, such as in sub-area A. Ultimately, when the underground coal fires die, such as in sub-area C, the CO₂/CO ratio is ~ 20 as the CO₂ concentration decreases. The volume ratio of CO₂/CO is not associated with vent temperature, but it appears related to geological conditions. The CO₂/CO ratio in the big vents is 88.57, but higher than in the small vents and cracks. It was suggested that well-ventilated areas have more rapid CO oxidation (Engle et al. 2012). In comparison with the vents and cracks, the mean CO₂/CO ratio in sub-area A is lower, and it may be because the low oxygen supply in sub-area A decreases combustion efficiency.

Effect of Underground Coal Fires on Soil Properties

Relation of Underground Coal Fires with Organic Matter Content

The spatial distribution of soil organic matter contents of the investigated areas is illustrated in Fig. 5. Soil color in the background area (B) is the lightest, with mean organic matter content of 20.83 mg/g. The distribution of organic matter con-

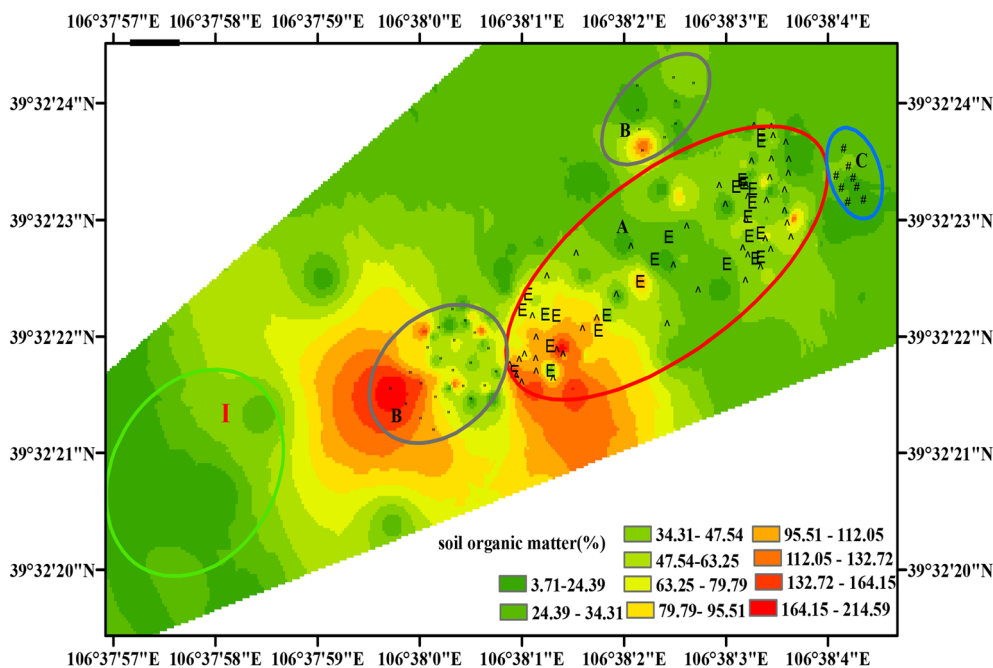


Figure 5. Distribution of organic matter content in soil of the investigated area.

content in the background area is close to normal distribution and mostly falls in the range of 12.13–25.62 mg/g (Fig. 5). Soil color in the coal fire area (II) is much darker than in the background area, and the mean value of organic matter contents is 76.38 mg/g, increasing significantly by 68.6% compared to that in the background area ($p < 0.01$). This indicates that the underground coal fires have a great influence on surface soil organic matter content. Soil organic matter contents in sub-area B are nearly 3.5 times higher than the background level (Fig. 5). Research showed that photosynthetic capacity can improve when CO₂ concentration in soil increases moderately (generally < 5%), or when vegetation withers and dies by root asphyxia (e.g., Derakhshan-Nejad et al. 2019). However, the CO₂ content in soil in sub-area B mostly falls in the range of 0.3–1.24% (Table 2). This illustrates that it was toxic gases (nitride, sulfide) emitted from the coal fire area that causes vegetation to degrade and die (Kuenzer et al. 2007), instead of CO₂.

Soil color depth in sub-area A, where the mean organic matter content is 73.19 mg/g (Fig. 6), is almost as same as in sub-area B. The difference of the means of soil organic matter content in sub-areas A and B is not statistically significant ($p > 0.05$), which illustrates that vegetation may have once existed in

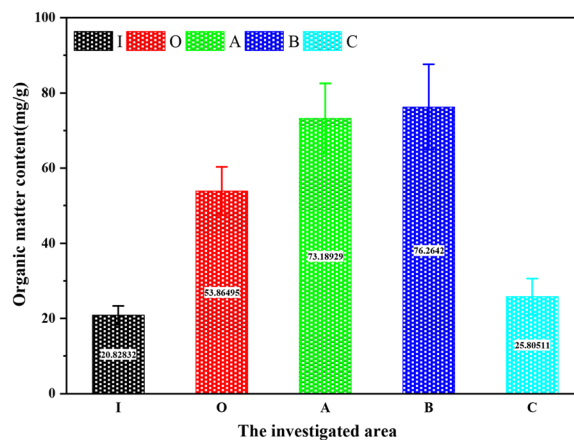


Figure 6. Organic matter content comparison of the investigated area.

sub-area A. Long-term underground coal fires damage surface vegetation, and surface litter is burned into black ash (Fig. 3A). Plant residues in soil are decomposed and then transformed to organic matter through erosion and leaching. In addition, organic residues, organic particles, and their carbonated particles mixed into the soil also result in

increase in soil organic matter to a certain extent (Cui et al. 2012; Zhao et al. 2016).

The color of surface soil covering the cracks and vents is lighter than in surrounding zones. The mean of soil organic matter contents in the vents/cracks area is 53.86 mg/g (Fig. 6), which is significantly reduced by 35.89% compared to that in sub-area A, and the surface temperature at vents and cracks is significantly higher than its surrounding zones (Table 2). These indicate that combustion intensity has significant effects on soil organic matter content. Organic carbon pyrolyzes under high temperature, and severe fire could render organic carbon to mineralize. In addition, leaching of soluble organic carbon and erosion of soil near the vents and cracks also result in decrease in soil organic matter content (Certini 2005; Liu et al. 2016). The mean of soil organic matter content in the coal fire area is lowest in sub-area C (Fig. 6), but slightly higher than in the background area. The possible reason for this is the long-term leaching of soluble organic carbon under acid conditions.

Relation of Underground Coal Fires with Soil pH

Figure 7 shows the spatial distribution of soil pH in the investigated area. The mean of soil pH in the coal fire area is 6.22, significantly lower by 18.5% compared to the background ($p < 0.01$). This indicates the underground coal fires have a significant effect on soil pH. The background area exhibits the highest soil pH (Fig. 7), mostly ranging from 7.6 to 8.0 (Fig. 7), confirming that soil in the Wuda District is alkaline (Liang 2018). Soil color is the deepest at the cracks and vents, where the minimum and mean soil pHs are 2.27 and 3.47, respectively (Fig. 7), thus indicating strong soil acidity in this area. Querol et al. (2011) investigated the pH and leachable content of trace elements in condensates from gaseous emissions in the vents and found that the strong acidity coincided with soil enriched in Al-, K-, Mg-, and Fe-bearing sulfates. The sources for the strong soil acidity may thus be attributed to: (a) hydrolysis of water by Fe and Al species and (b) oxidation of SO_2 ($\text{SO}_2 + 3/2\text{O}_2 + \text{H}_2\text{O} = \text{SO}_4^{2-} + 2\text{H}^+$). Therefore, some aqueous equilibria, such as Fe^{3+} - $\text{Fe}(\text{OH})^{2+}$, Al^{3+} - $\text{Al}(\text{OH})^{2+}$, Al^{3+} - $\text{Al}(\text{OH})_2^+$, and HSO_4^- - SO_4^{2-} , can maintain strong soil acidity.

Soil salt contents at the vents and crack are significantly higher than in the other areas (Fig. 8).

In addition, a negative correlation exists between soil SO_2 content and soil pH ($R^2 = -0.82$, $p < 0.01$) (Fig. 9). Therefore, we propose one possible explanation for the formation of strong soil acidity at the vents and cracks, namely: gaseous SO_2 in soil, existing as adsorption or free state, reacts with moisture in soil or air to form sulfite or even sulfuric acid. Gaseous organic and inorganic species emitted from the vents and cracks interact with sulfuric acid and give rise to sulfur-bearing minerals as temperature decreases. The mixture of sulfur-bearing minerals (e.g., Ca^{2+} , NH_4^+ , Al^{3+} , K^+ , Mg^{2+} , and Fe^{3+} sulfates) with soil increases soil salt content, and soil salt enriched in Al-, K-, Mg-, and Fe-bearing sulfates results in strong soil acidity.

Soil color in sub-area A is relatively light and shows soil pH in the 5.42–7.32 range (Fig. 7), with mean of 6.4 (Fig. 7). Soil pH is closely related to SO_2 and CO_2 contents (Fig. 9), indicating that SO_2 and CO_2 intrusion may have led to soil acidification in sub-area A. In addition, Hong (2018) found good correlation between soil SO_4^{4-} content and dust pH in the Wuda coalfield, suggesting that acids in soil likely exist in the form of acid sulfates (KHSO_4 or NaHSO_4). However, SO_2 contents are minor compared to CO_2 in sub-area A, and so CO_2 likely plays an important role in soil acidification. CO_2 can react with soil water, and then H^+ and HCO_3^{3-} ionized in soil aqueous solution can acidify pore water in soil (Wei et al. 2015). HCO_3^- - H^+ equilibria may be responsible for pH values around 6. Whether the soil acidification in sub-area A is caused mainly by SO_2 or CO_2 needs further study. Soil pH in sub-area C is high, and soil color there is nearly the same as in the background (Fig. 7). The mean soil pH in sub-area B is 7.55, and this has no significant difference with that in the background area (Fig. 8). This is because CO_2 contents in soil in sub-area B are lower than in sub-area A, where SO_2 is not detected (Table 2). As for sub-area C, where soil pH ranges mostly from 3.84 to 5.9 and thus shows moderate acidity (Fig. 7), soil color is close to that in sub-area A. Therefore, soil pH is reliably related to the underground coal fires. Soil tends to be moderate acidic or even strong acidic in the high-temperature zone with obvious features and in the extinguished area, whereas soil seems to be neutral in the surroundings of the high-temperature zone. Soil pH nearly remains unchanged in the area less affected by coal fires.

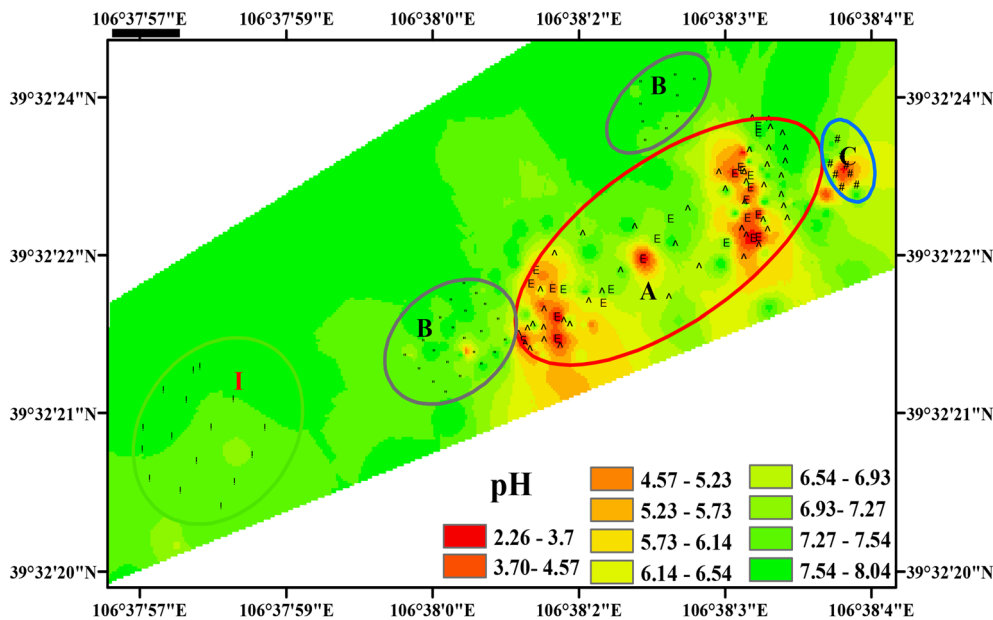


Figure 7. Distribution of soil pH in the investigated area.

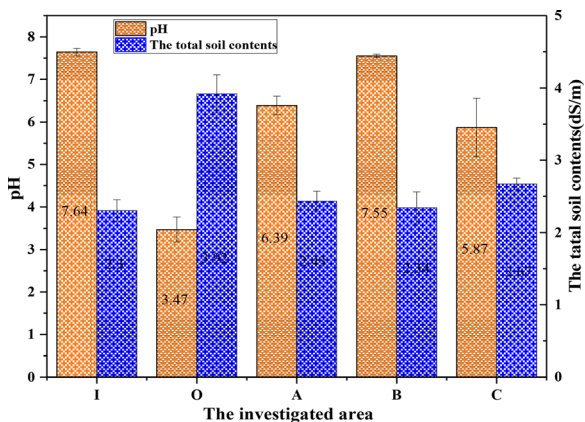


Figure 8. Comparison of soil pH and total salt content in the investigated area.

CONCLUSIONS

The integrated surveys conducted in the coal fire area of Wuda comprise analyses of surface soil emitted gases and soil chemistry properties (e.g., soil pH, soil organic matter content, total salt content). The distribution of the concentration and the composition of the emitted gas vary from the coal fire

areas, and the statistical t-test reveals that the underground coal fires are statistically significant ($p < 0.01$) for the soil pH and the organic matter. The following conclusions are reached.

Thermal surface anomalies are dominant mainly at vents and cracks. The surface temperature correlated with soil gas contents at the cracks and vents, whereas there is no correlation between surface temperature and soil gas content due to solar heating in sub-area A. The mutual correlations among emitted gases in soil in sub-area A are similar to those in the vents and cracks, which indicate that their generation mechanism is the same and that there is existence of microseepage from the high-temperature zone underground.

The gases CO_2 , CO , and CH_4 are dominant in the coal fire area, whereas SO_2 , H_2S , C_2H_6 , C_2H_4 , and C_2H_2 can be detected only in the high-temperature zone. In sub-area C, small amounts of H_2 and CO can be still detected, while its soil contents of CO_2 and CH_4 are close to those in the background area. A portion of CH_4 and CO_2 in sub-area B may have been generated by respiration of plant roots and by decomposition of microorganisms. The volume ratio of CO_2/CO varies with degree of the underground fires, and coincides with subsurface geological features.

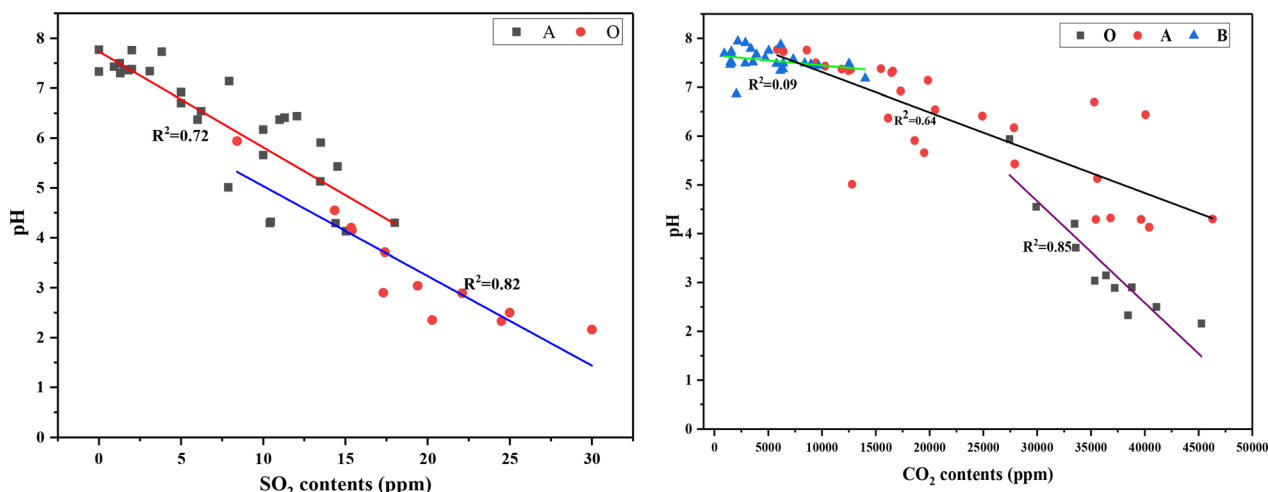


Figure 9. Correlations of SO₂ and CO₂ contents with soil pH.

The underground coal fires can raise the organic matter contents through mixing of organic residues, organic particles, and their carbonated particles with the soil. However, the severe fires can cause a significant removal of organic matter through pyrolysis, leaching, and erosion. The underground coal fires can reduce soil pH, and the strong soil acidity correlates with the sulfate contents in soil at the vents and cracks. Soil pH correlated with CO₂ and SO₂ contents in soil in sub-area A, and the long-term CO₂ and SO₂ exposure in soils may have resulted in the acidification of pore water in the soils. Soil organic matter content and soil pH are related to the degree of underground coal fires. It is recommended that they, in combination with emitted gas emissions, have potential to be used as indicators of high-temperature resource. However, the anomaly of chemical soil properties in the coal fire area may change with soil type, combustion intensity, vegetation density, and coal rank.

ACKNOWLEDGMENTS

This work was supported by National Natural Science Foundation of China (No. 51874313) and National Key R&D Program of China (No. 2018YFC0808101). We are grateful to Dr. Jim Hower and an anonymous reviewer for their valuable comments, and we are thankful to Dr. John Carranza's efficient editing.

REFERENCES

- Carras, J. N., Day, S. J., Saghafi, A., & Williams, D. J. (2009). Greenhouse gas emissions from low-temperature oxidation and spontaneous combustion at open-cut coal mines in Australia. *International Journal of Coal Geology*, 78(2), 161–168.
- Certini, G. (2005). Effects of fire on properties of forest soils: a review. *Oecologia*, 143(1), 1–10.
- Cui, X. Y., Hao, J. M., Zhao, S. S., Sang, Y., Wang, H. Q., & Di, X. Y. (2012). Temporal and spacial changes of total soil organic carbon content as affected by an experimental forest fire in the Greater Xing's a mountain. *Journal of Soil and Water Conservation*, 26(5), 195–200.
- Dai, S. F., Ren, D. Y., Tang, Y. G., Shao, L. Y., & Li, S. S. (2002). Distribution, isotopic variation and origin of sulfur in coals in the Wuda coalfield, Inner Mongolia, China. *International Journal of Coal Geology*, 51(4), 237–250.
- Derakhshan-Nejad, Z., Sun, J., Yun, S.-T., & Lee, G. (2019). Potential CO₂ intrusion in near-surface environments: a review of current research approaches to geochemical processes. *Environmental Geochemistry and Health*, 41(5), 2339–2364.
- Engle, M. A., Radke, L. F., Heffern, E. L., O'Keefe, J. M. K., Hower, J. C., Smeltzer, C. D., et al. (2012). Gas emissions, minerals, and tars associated with three coal fires, Powder River Basin, USA. *Science of the Total Environment*, 420, 146–159.
- Engle, M. A., Radke, L. F., Heffern, E. L., O'Keefe, J. M. K., Smeltzer, C. D., Hower, J. C., et al. (2011). Quantifying greenhouse gas emissions from coal fires using airborne and ground-based methods. *International Journal of Coal Geology*, 88(2–3), 147–151.
- Garrison, T., O'Keefe, J. M. K., Henke, K. R., Copley, G. C., Blake, D. R., & Hower, J. C. (2017). Gaseous emissions from the Lotts Creek coal mine fire: Perry County, Kentucky. *International Journal of Coal Geology*, 180, 57–66.
- Harvey, O. R., Qafoku, N. P., Cantrell, K. J., Lee, G., Amonette, J. E., & Brown, C. F. (2013). Geochemical implications of gas leakage associated with geologic CO₂ storage—a qualitative review. *Environmental Science and Technology*, 47(1), 23–36.

- Hong, X. P. (2018). Fluorine and acid pollutant within soil around three coal-rich areas in China. China University of Mining and Technology (Beijing), Beijing (PhD Thesis).
- Hower, J. C., Henke, K., O'Keefe, J. M. K., Engle, M. A., Blake, D. R., & Stracher, G. B. (2009). The Tiptop coal-mine fire, Kentucky: Preliminary investigation of the measurement of mercury and other hazardous gases from coal-fire gas vents. *International Journal of Coal Geology*, 80(1), 63–67.
- Hower, J. C., O'Keefe, J. M. K., Henke, K. R., Wagner, N. J., Copley, G., Blake, D. R., et al. (2013). Gaseous emissions and sublimates from the Truman Shepherd coal fire, Floyd County, Kentucky: A re-investigation following attempted mitigation of the fire. *International Journal of Coal Geology*, 116–117, 63–74.
- Kuenzer, C., & Stracher, G. B. (2012). Geomorphology of coal seam fires. *Geomorphology*, 138(1), 209–222.
- Kuenzer, C., Zhang, J., Tetzlaff, A., van Dijk, P., Voigt, S., Mehl, H., et al. (2007). Uncontrolled coal fires and their environmental impacts: Investigating two arid mining regions in north-central China. *Applied Geography*, 27(1), 42–62.
- Liang, Y. C. (2018). Emission characteristics of typical pollutants of coal fire in Wuda, Inner Mongolia. China University of Mining and Technology (Beijing), Beijing (PhD Thesis).
- Liu, F. L., Xiao, H. H., & Luo, P. F. (2016). A Review: the effect of forest fire on soil organic matter. *Chinese Journal of Soil Science*, 47(1), 239–245.
- Melody, S. M., & Johnston, F. H. (2015). Coal mine fires and human health: What do we know? *International Journal of Coal Geology*, 152, 1–14.
- O'Keefe, J. M. K., Henke, K. R., Hower, J. C., Engle, M. A., Stracher, G. B., Stucker, J. D., et al. (2010). CO₂, CO, and Hg emissions from the Truman Shepherd and Ruth Mullins coal fires, eastern Kentucky, USA. *Science of the Total Environment*, 408(7), 1628–1633.
- O'Keefe, J. M. K., Neace, E. R., Hammond, M. L., Hower, J. C., Engle, M. A., East, J., et al. (2018). Gas emissions, tars, and secondary minerals at the Ruth Mullins and Tiptop coal mine fires. *International Journal of Coal Geology*, 195, 304–316.
- Querol, X., Zhuang, X., Font, O., Izquierdo, M., Alastuey, A., Castro, I., et al. (2011). Influence of soil cover on reducing the environmental impact of spontaneous coal combustion in coal waste gobbs: A review and new experimental data. *International Journal of Coal Geology*, 85(1), 2–22.
- Rasheed, M. A., Lakshmi, M., Rao, P. L. S., Kalpana, M. S., Dayal, A. M., & Patil, D. J. (2013). Geochemical evidences of trace metal anomalies for finding hydrocarbon microseepage in the petroliferous regions of the Tatipaka and Pasarlapudi areas of Krishna Godavari Basin, India. *Petroleum Science*, 10(1), 19–29.
- Sechman, H., Kotarba, M. J., Fiszer, J., & Dzieniewicz, M. (2013). Distribution of methane and carbon dioxide concentrations in the near-surface zone and their genetic characterization at the abandoned “Nowa Ruda” coal mine (Lower Silesian Coal Basin, SW Poland). *International Journal of Coal Geology*, 116–117, 1–16.
- Shan, B., Wang, G., Cao, F., Wu, D., Liang, W., & Sun, R. (2019). Mercury emission from underground coal fires in the mining goaf of the Wuda Coalfield, China. *Ecotoxicol Environ Saf*, 182, 109409.
- Sokol, E. V., Novikova, S. A., Alekseev, D. V., & Travin, A. V. (2014). Natural coal fires in the Kuznetsk Coal Basin: Geologic causes, climate, and age. *Russian Geology and Geophysics*, 55(9), 1043–1064.
- Song, Z., Huang, X., Jiang, J., & Pan, X. (2020a). A laboratory approach to CO₂ and CO emission factors from underground coal fires. *International Journal of Coal Geology*. <https://doi.org/10.1016/j.coal.2019.103382>.
- Song, Z., Huang, X., Kuenzer, C., Zhu, H., Jiang, J., Pan, X., et al. (2020b). Chimney effect induced by smoldering fire in a U-shaped porous channel: A governing mechanism of the persistent underground coal fires. *Process Safety and Environmental Protection*, 136, 136–147.
- Song, Z., & Kuenzer, C. (2014). Coal fires in China over the last decade: A comprehensive review. *International Journal of Coal Geology*, 133, 72–99.
- Song, Z., & Kuenzer, C. (2017). Spectral reflectance (400–2500 nm) properties of coals, adjacent sediments, metamorphic and pyrometamorphic rocks in coal-fire areas: A case study of Wuda coalfield and its surrounding areas, northern China. *International Journal of Coal Geology*, 171, 142–152.
- Song, Z., Kuenzer, C., Zhu, H., Zhang, Z., Jia, Y., Sun, Y., et al. (2015). Analysis of coal fire dynamics in the Wuda syncline impacted by fire-fighting activities based on in situ observations and Landsat-8 remote sensing data. *International Journal of Coal Geology*, 141–142, 91–102.
- Song, Z., Wu, D., Jiang, J., & Pan, X. (2019). Thermo-solutal buoyancy driven air flow through thermally decomposed thin porous media in a U-shaped channel: Towards understanding persistent underground coal fires. *Applied Thermal Engineering*. <https://doi.org/10.1016/j.applthermaleng.2019.113948>.
- Stracher, G. B., & Taylor, T. P. (2004). Coal fires burning out of control around the world: thermodynamic recipe for environmental catastrophe. *International Journal of Coal Geology*, 59(1–2), 7–17.
- Wang, G., Cao, F., Shan, B., Meng, M., Wang, W., & Sun, R. (2019). Sources and assessment of mercury and other heavy metal contamination in soils surrounding the Wuda underground coal fire area, inner Mongolia, China. *Bulletin of Environmental Contamination and Toxicology*, 103(6), 828–833.
- Wang, Y., Li, X., Wang, W., & Guo, Z. (2017a). Experimental and in situ estimation on hydrogen and methane emission from spontaneous gasification in coal fire. *International Journal of Hydrogen Energy*, 42(29), 18728–18733.
- Wang, Y., Wu, J., Xue, S., Wang, J., & Zhang, Y. (2017b). Experimental study on the molecular hydrogen release mechanism during low-temperature oxidation of coal. *Energy & Fuels*, 31(5), 5498–5506.
- Wei, Y., Córdoba, P., Caramanna, G., Maroto-Valer, M., Nathaniel, P., & Steven, M. D. (2015). Influence of a CO₂ long term exposure on the mobilisation and speciation of metals in soils. *Geochemistry*, 75(4), 475–482.
- Xu, W. P., Wang, G. J., Cheng, T. J., Zhao, K. B., & Tang, Y. P. (2017). Mechanisms of geochemical anomalies in prospecting for oil and gas based on laboratory simulation of microseepage. *Acta Petroli Sinica*, 3, 72–82.
- Zeng, Q., Dong, J. X., & Zhao, L. H. (2018). Investigation of the potential risk of coal fire to local environment: A case study of Daquanhu coal fire, Xinjiang region, China. *Science of the Total Environment*, 640–641, 1478–1488.
- Zhang, J., & Kuenzer, C. (2007). Thermal surface characteristics of coal fires 1 results of in situ measurements. *Journal of Applied Geophysics*, 63(3–4), 117–134.
- Zhang, T., Xu, J., Zeng, J., & Lou, K. (2013). Diversity of prokaryotes associated with soils around coal-fire gas vents in MaNasi county of Xinjiang, China. *Antonie Van Leeuwenhoek*, 103(1), 23–36.
- Zhang, J. M., et al. (2008). *Underground coal fires in China: Origin, detection, fire-fighting, and prevention* (1st ed.). Beijing: China coal industry publishing house.
- Zhao, Z. X., Li, Z. C., Zhou, J. G., Cheng, C. F., Zhao, R. Y., & Sun, J. J. (2016). Effect of fire on soil organic carbon of natural Pinus massoniana forest in north subtropical area of China. *Chinese Journal of Ecology*, 35(1), 135–140.